Journal of Alloys and Compounds 638 (2015) 289–297

Contents lists available at ScienceDirect

Journal of Alloys and Compounds

journal homepage: www.elsevier.com/locate/jalcom

Synthesis of vanadium pentoxide (V_2O_5) nanobelts with high coverage using plasma assisted PVD approach

Rabindar K. Sharma *, Prabhat Kumar, G.B. Reddy

Thin Film Laboratory, Department of Physics, Indian Institute of Technology, Delhi, New Delhi 110016, India

ARTICLE INFO

Article history:
Received 13 November 2014
Received in revised form 16 February 2015
Accepted 25 February 2015
Available online 3 March 2015

Keywords:
Vanadium pentoxide
Plasma assisted growth
Nanobelts
Oxygen plasma

ABSTRACT

Cost-saving, easy-handling, and eco-affable plasma assisted sublimation process (PASP) is proposed to synthesize vanadium pentoxide (V_2O_5) nanobelts (NBs) with excellent coverage on Si [100] wafer using oxygen plasma without using surfactants/catalysts. Pure orthorhombic V_2O_5 NBs having average length of few hundred of microns with quite uniform width nearly of 100 nm are formed at 500 °C. No film is deposited on Si in presence of oxygen gas without exciting plasma at 500 °C. HRTEM analysis with SAED pattern confirm that all V_2O_5 NBs are single crystalline in nature with the fringe width of 0.33 nm corresponding to [010] crystal plane. The XPS analysis shows the compositional purity and sub-stoichiometric nature of V_2O_5 NBs. The sub-stoichiometric nature of NBs is manifested through an appearance of low intensity peak corresponding to low oxidation state of V (i.e. V^{4+}) at the binding energy of 514.8 eV. The micro-Raman and FTIR analysis of NBs are carried out to study the different vibrational modes exhibited by V and O atoms coordinated in distinct fashions. The nanobelts exhibit room temperature PL emission in UV–visible realm with a broad hump in the range of 450–750 nm, which confirms the presence of oxygen defects in NBs and strongly supports the XPS results as well. The possible growth mechanism of α-V_2O_5 NBs is proposed in this paper briefly.

1. Introduction

One-dimensional materials have remarkably great attention in the past decade owing to their sophisticated and excellent physical and chemical properties compare to their bulk counterparts. Nowadays, primarily the current research focused on the synthesis of nanomaterials has rapidly extended with controlling the shape of materials and understanding the correlations between the material properties and their nanostructures of different surface morphologies [1,2]. Among them, one dimensional nanostructures of V_2O_5 have been extensively studied in recent years owing to their potential applications in chemical sensors [3], field emitters [4], catalysts [5], lithium ion batteries [6], and electrochromic [7] and other nanodevices. It is reported that vanadium oxides have several stoichiometries including V_2O_3, VO_2, and V_2O_5 in different phases. V_2O_3 has a paramagnetic metallic phase of corundum structure (Al_2O_3), and is an antiferromagnetic insulator of monoclinic structure at temperatures above or below than 165 K, respectively. VO_2 is an interesting narrow band gap (i.e. 0.7 eV) semi conducting material, which undergoes a semiconductor to metal phase transition (i.e. from monoclinic phase to tetragonal phase) at 68 °C, resulting in giant drops of its electrical resistance and transmittance of infrared signal [8]. Orthorhombic phase of vanadium oxide (α-V_2O_5) is the most stable oxide and have tremendous research interest in the past years due to their excellent chemical and physical properties. Especially the multi valence nature, layered structure, and excellent thermoelectric property are making vanadium pentoxide a fascinating material for nano-device fabrication prospective [9]. Vanadium atom occupies the highest oxidation state in orthorhombic phase of V_2O_5, which has V—O bonding system and crystallizes with an orthorhombic unit cell structures belonging to the P_{mnm} space group. The lattice parameters of α-V_2O_5 are specified as $a = 11.50$ Å, $b = 3.56$ Å, and $c = 4.369$ Å [10]. It has well-defined layered structure, which built up from distorted trigonal bi-pyramidal coordinated polyhedra of V atoms surrounded by O atoms, that contribute their edges to form $(V_2O_4)_n$ zigzag double chains along the (001) direction and are cross linked along (100) direction through shared corners. These distorted polyhedra in V_2O_5 have a short vanadyl bond (~1.58 Å) and four O atoms positioned in basal plane at bond lengths ranging from 1.78 to 2.02 Å. The sixth O atom in the coordinated polyhedra of V atom lies along vertical axis opposite to V—O bond at a bond length of 2.79 Å [10]. From chemical applications point of view, α-V_2O_5 is an excellent catalyst because of its

* Corresponding author. Tel.: +91 1126591353; fax: +91 1126581114.
E-mail address: rkrksharma6@gmail.com (R.K. Sharma).

http://dx.doi.org/10.1016/j.jallcom.2015.02.178
0925-8388/

generative and diverse chemistry that is based on two factors, namely the variety of vanadium oxidation states ranging from 2^+ to 5^+ and the geometrical variability of atomic oxygen coordination [9]. The latter comprise octahedra, pentagonal by-pyramids, square pyramids, and tetrahedra, which might be combined with shared corners, faces and edges conceding an impressive variety of structural arrangements. This structural richness is responsible to the origin of differently coordinated oxygen ions, which render the crucial ingredient for the physical and chemical surface studies. To date, variety of physical and chemical vapor deposition techniques such as thermal evaporation, sputtering, pulsed laser deposition, and sol–gel method have been employed to synthesize variety vanadium oxidesnanostructures. Diaz-Guerra et al. [11] have reported the growth of V_2O_5 nanowires and nanotips by thermal evaporation on 4H—SiC and Si substrate without using catalyst. Rui et al. [12] published a report based on the growth of ultra-thin hydrated vanadium pentoxide single crystalline nanosheets by the sol–gel process. Zhai et al. [13] reported the fabrication of centimeter-long V_2O_5 nanowires through a hydrothermal route accompanied with thermal treatment process. Lim et al. [14] obtained nano crystalline vanadium oxide thin films on variety of substrate using plasma assisted reactive RF-sputtering process. Beside those as listed above, many other research groups have used several synthesis approaches either individual or followed by some post deposition treatments to form the variety of nanostructures on different substrates. Although these routes are effective from the growth point of view, but have their short comings. Many of PVD routes required templates/surfactants, very high order of vacuum and temperature, whereas the chemical routes are relatively more complex, produce contaminations and toxic gases as well. The properties of deposited V_2O_5 films are mainly depend not only on the deposition process but also on processing parameters such as deposition/growth temperature, deposition time, and oxygen partial pressure in vacuum chamber during deposition. In this contribution, we report the large scale growth of purely orthorhombic V_2O_5 NBs on Si [100] substrate employing a facile PVD process called plasma assisted sublimation process (PASP) without using any surfactant/catalyst for the first time to the best of authors knowledge. Resistively heated vanadium metal strip is used as a source of sublimated V_2O_5 vapor throughout entire deposition. The morphological, structural, optical, compositional and vibrational studies of V_2O_5 nanobelts are discussed systematically in this paper. The observed structural and morphological results endorse that the crystallinity and surface microstructure of V_2O_5 films is strongly depending on growth temperature particularly in presence of oxygen plasma. The optimum temperature to grow V_2O_5 NBs with uniform coverage is 500 °C. No film is deposited on Si wafer in presence of simple oxygen gas without exciting plasma even the growth temperature is maintained at 500 °C. The HRTEM and SAED analysis of NBs reveal the single crystalline nature of NBs and closely consistent the XRD results as well. The detailed vibrational study of NBs is discussed using Raman and IR spectroscopies. The intense and broad PL emission of V_2O_5 NBs, ascertain the improvement in the degree of crystallinity with relatively better stoichiometric ratio. The vapor–solid (VS) approach is proposed to elaborate the formation of V_2O_5 NBs with the relevant growth model.

2. Experimental details

Vanadium pentoxide NBs have deposited on ultrasonically cleaned Si [100] substrates using remarkably efficient route called plasma assisted sublimation process (PASP). Two electrodes system is used to create oxygen plasma in vacuum chamber and schematic representation of complete experimental setup has been given in Ref. [15]. First, all the silicon substrates were cleaned supersonically in acetone, alcohol, and de-ionized water baths in sequences and then dried with a gentle nitrogen blow. After cleaning, silicon substrate is mounted on the rectangular shape vanadium strip (taking as a sublimation source) and gradually increasing the strip temperature with the rate of 2 °C/s up to the required temperature by suitably adjusting the current passes through it. In the present work, the films are deposited on three different substrate temperatures 300 °C, 400 °C and 500 °C. Thermocouple arrangement is fixed inside deposition chamber to record the substrate temperature continuously during growth. No temperature gradient is obtained between the upper (where the deposition is taking place) and lower surfaces of silicon substrate. The optimum ratio of substrate area $(1.5 \times 1.0)\,cm^2$ to that of the V strip $(8 \times 2)\,cm^2$ was found approximately of 1/9 to get uniform deposition on relatively large scale with uniform coverage density. The silicon substrate along with the sublimation source (V strip) is placed in between the electrodes in such a fashion that both are exposed completely in oxygen plasma. First, the vacuum chamber was evacuated up to 7.5×10^{-6} Torr, after that 99.9% pure oxygen was inserted in chamber to maintain the level of chamber pressure at 7.5×10^{-2} Torr and then switched on power to excite plasma between electrodes. The optimum values of electrode separation and plasma voltage are maintained constant at 7.5 cm and 2500 V, respectively during deposition. Once a stable oxygen plasma is established between electrodes then the V-strip is heated up to the desired value of temperatures. The deposition duration for all samples remains fixed as 30 min. The surface microstructures of all films are studied with scanning electron microscope (ZEISS-EVO Series scanning electron microscope model EVO-50). To record the surface topography with SEM, the samples are mounted on holder and a thin layer of gold is deposited to avoid charging owing to probing electron beam. Structural analysis of V_2O_5 nanobelts is studied using Philips X-ray diffractometer using Cu Kα radiation ($\lambda \sim 1.54$ Å) with a glancing angle kept constant at 1°. All the diffractograms are recorded in 2θ range of 10–60°, by using X-rays generated by electron beam current of 40 mA and accelerating voltage 45 kV. To study the vibrational properties of V_2O_5 NBs, micro-Raman spectroscopy of Renishaw-inVia (excited with Ar^+ line at 514.5 nm) and Perkin Elmer (Spectrum BX2) FTIR spectroscopy are employed in the spectral range from 200 to 1000 cm^{-1} and 400 to 1500 cm^{-1} respectively, with the resolution limit of 1 and 4 cm^{-1}. For the dimensional and the structural analysis, (TEM) micrographs of NBs are recorded using Philips Model CM12 operated at 120 kV with selected area electron diffraction (SAED) pattern. The specimens for TEM measurement are prepared by suspending the deposited films in ethanol and placing some droplets of this solution onto the standard carbon supported 600 mesh copper grid and drying them slowly. Further more insight characterization is performed using high-resolution transmission electron microscopy (HRTEM) to study the crystalline status of NBs. X-ray photoelectron spectroscopic (XPS) studies are performed using Perkin Elmer Model PHI 1257 spectrometer, with anode Mg/Al 25 kV X-ray source of power 150 Watts with the resolution of 0.2 eV. The radiation used in XPS in present study is Al Kα radiation. The probing X-ray photons are incident at an angle of 45° relative to the normal of substrate and the rotational axis of hemispherical analyzer was parallel to the substrate normal. The photoluminescence (PL) measurements of NBs was performed using Horiba Jobin Yvon spectroflourometer (Flurolog III) with xenon lamp of power 450 Watts taken as a source and R928P photomultiplier tube in photo counting mode as detector. All measurements are performed at room temperature.

3. Results and discussion

3.1. Structural analysis

X-ray diffractograms (XRD) are recorded to investigate the composition and phase purity of V_2O_5 thin films deposited in O_2-plasma ambiance for 30 min as a function of growth temperature, can be seen in Fig. 1. The sharp and intense diffraction peaks in all samples deposited at different temperatures are endorsed the polycrystalline nature of films and confirmed the existence of nanostructures. All the diffraction peaks in XRD pattern of films can be unambiguously indexed according to the pure orthorhombic crystalline phase of V_2O_5, which are precisely corresponding to the standard value as reported in JCPDS file (89-0612) with the lattice constants of $a = 11.48$ Å, $b = 3.55$ Å, and $c = 4.36$ Å and no traces of other characteristics peaks corresponding to impurity phases is detected under the limit of resolution [4]. The prominent increase in intensity and sharpness of peaks with substrate temperature acknowledged the betterment in degree of crystallinity (see in Fig. 1). As the deposition temperature increases from 300 to 400 °C the peak intensity associated to [101] and [010] crystal planes positioned at 2θ values 20.35° and 26.22° respectively, get significantly enhanced in compare to other peaks, which indicating that nanostructures are growing prominently along these crystallographic directions (see in Fig. 1b and c). On further increase in temperature up to 500 °C, sample exhibits most intense peak

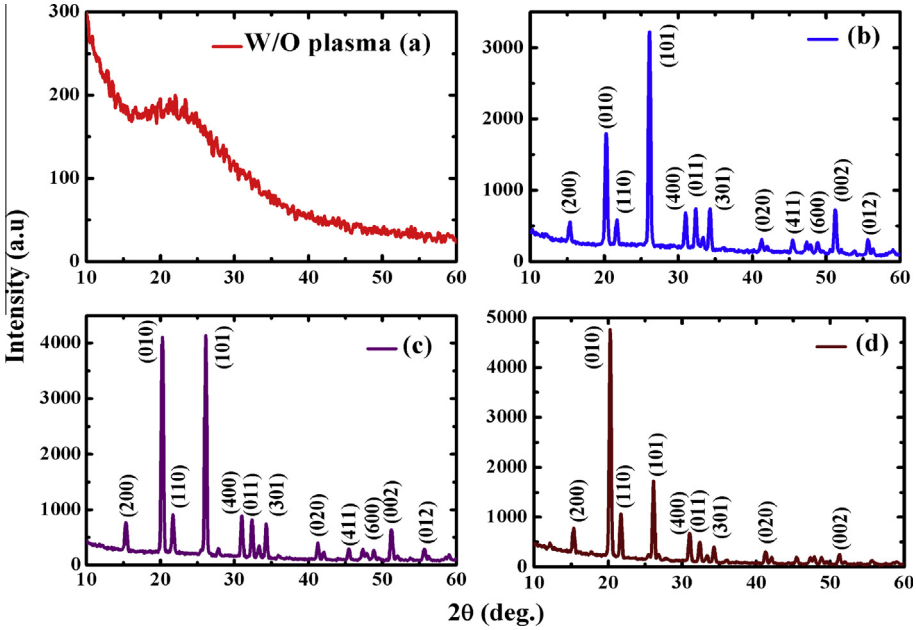

Fig. 1. X-ray diffractograms of V_2O_5 thin films (a) deposited at 500 °C without O_2-plasma, (b) deposited at temperature 300 °C in O_2-plasma, (c) at 400 °C in plasma and (d) at 500 °C in O_2-plasma.

correspond to [0 1 0] crystal plane, manifested that nanostructured thin film is growing preferentially along *b*-direction (see in Fig. 1c). Beside that it is worth noting that no diffraction peaks are found in sample kept on V-metal in oxygen gas without exciting plasma at 500 °C. At this temperature even the metal would oxidized but the oxide molecules will not reach on substrate without plasma, can be seen in Fig. 1a. Hence the presence of O_2-plasma must be required to grow uniform V_2O_5 film on entire substrate. The estimated mean crystallite size of films deposited at the assumed temperature is found to be 26.5, 28.8, and 30.6 nm, respectively. The crystallite size are calculated by considering the diffraction planes having maximum intensities using the Debye–Scherrer formula. The relatively larger crystallite size at 500 °C assured its better crystallinity than other films deposited at lower temperatures, which surmised that growth temperature is strongly determine the degree of crystallinity of films.

3.2. Surface morphological studies

Fig. 2 shows the surface micrographs of V_2O_5 thin films fabricated on Si [1 0 0] substrates using PASP under different ambient at constant growth temperature 500 °C. First, in order to investigate the effect of oxidizing media on film growth, two different ambient viz. normal oxygen gas and O_2-plasma ambience at the same vacuum level are used. The SEM micrograph of film deposited in normal oxygen atmosphere exhibits completely smooth surface, no matter the value of growth temperature in the considered operating range 300–500 °C (see in Fig. 2a). Since, it has been reported earlier [15,16] that the presence of O_2-plasma not only facilitating in oxidation of metallic strip (V-metal strip) at relatively lower temperature but also directing the V_2O_5 molecules to reach on to substrates and distribute these over the large area of substrate ($1.5 \times 1.5\ cm^2$) in homogenous fashion. In absence of O_2-plasma even the oxidation of vanadium metal is occurring at 500 °C but the detached molecular species are not properly directed onward to substrates from V-metal, resulting in no film deposition is taking place. This confirmed the importance of O_2-plasma for the growth of V_2O_5 nanostructured thin film with good coverage density. The obtained SEM result in absence of O_2-plasma is completely agreed with the XRD findings. Secondly, to study the surface modifications of films as a function of growth temperature in O_2-plasma, the SEM micrographs are recorded systematically in Figs. 2 and 3. The sample prepared at 300 °C reveals the formation of spherically shaped particles accompanied with few number of NBs having rectangular cross-section (inset of Fig. 2b). The average diameters of these particles are ranging in 50–400 nm, while the existing belts having average length in the order of few microns. All these NBs at this temperature are uniform along its whole length with the average width of the order of ~100 nm. As the temperature increases at 400 °C, relatively larger amount of V_2O_5 vapor detached from metallic strip during oxidation and reaches on substrate, resulting in the spherical shaped particle transform their shape in almost rectangular form as can be seen in Fig. 2c. The continuous arrival of V_2O_5 vapor flux on substrate allowed these particles to start coalescence parallelly with other particles those located in vicinity during re-crystallization. It is difficult to estimate the exact particle length owing to the complete merging of these particles with other neighboring particles, but the width of these particles can be measured. The width of a single particle is found to be nearly 200 nm. The inset in Fig. 2c is demonstrated the combined width of ~400 nm of two parallelly merged particles. The film deposited at 500 °C shows V_2O_5 NBs with well-defined facets and rectangular cross section is depicted in Fig. 3. The surface microstructure is quite uniform confirming that the growth is flourished uniformly on the entire substrate, which attributing to the uniform thickness of deposited film on the entire area of substrate, see in Fig. 3a and b. The average length and the width of NBs are estimated to be of the order of few hundred of microns and 400 nm, respectively (see in Fig. 3c). Since, all the silicon substrates are placed directly on sublimation source during growth, leads to a little thermal gradient between upper and the lower faces of silicon substrates almost at all temperature values. As the growth temperature is reached at 500 °C, detached oxide vapor flux reaching on to the substrate is relatively more than previous cases, which allowing anisotropic growth on the top edge of nanobelts but no nucleation is taking place on sides, consequently the growth is completely focused only in a single direction. It is supposed the existence of the oxygen vacancies at top edges of NBs grown in oxygen plasma offered the nucleation spot for the further

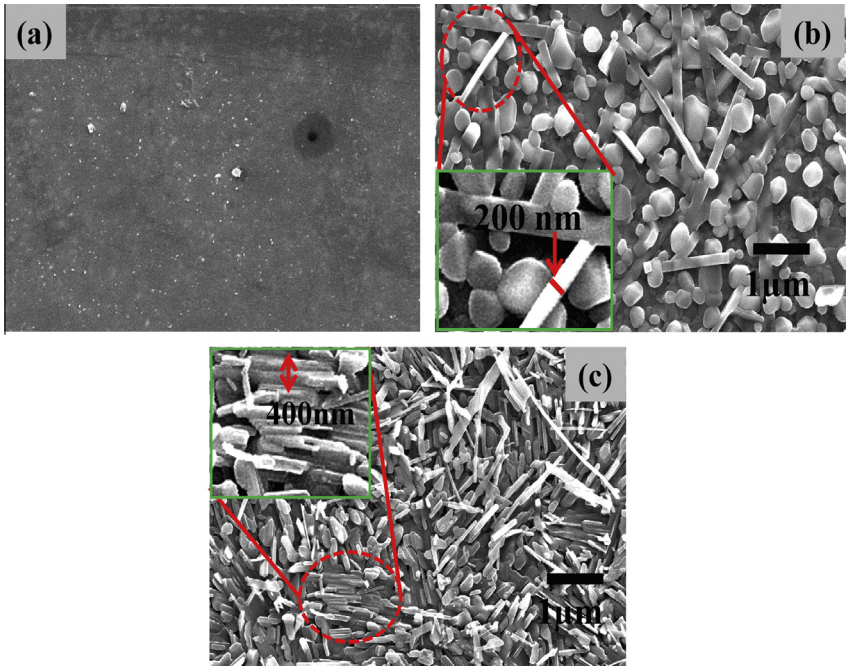

Fig. 2. SEM micrographs of V_2O_5 thin films at low magnification (a) deposited at 500 °C without O_2-plasma, (b) deposited at temperature 300 °C in O_2-plasma and (c) at 400 °C in plasma.

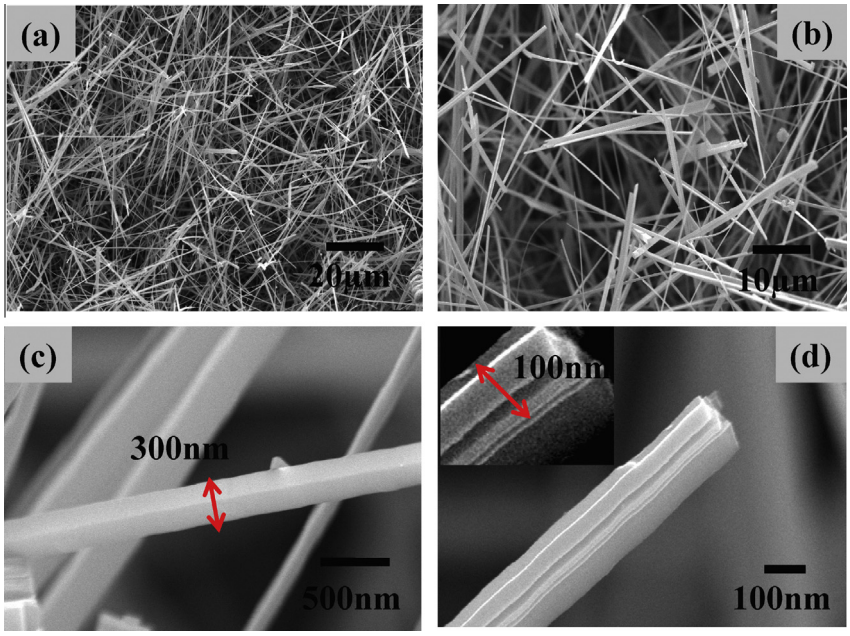

Fig. 3. SEM micrographs of V_2O_5 thin films formed at 500 °C on different magnification in O_2-plasma (a and b) formation of V_2O_5 NBs with high coverage, (c) shows uniform width ~300 nm and (d) shows parallelly attached NBs having combined thickness ~ 100 nm.

incoming V_2O_5 molecules to condense. This will also promote the growth of V_2O_5 NBs with very high aspect ratio. This high aspect ratio of NBs is suggested that the belts are rapidly growing along its length compare to the other directions. A closely examined SEM image at higher magnification revealed that most of the NBs are not individual or single but composed with parallelly aligned NBs having different thicknesses. The combined thickness of nanobelt is estimated nearly 100 nm (see in Fig. 3d). It should be noted that the width of NBs almost has no change after coalescence with other nanobelts. All the SEM results are altogether in accord with XRD outcomes. So finally, it can be concluded that O_2-plamsa accompanied with appropriate growth temperature (500 °C) is most required to grow V_2O_5 NBs on Si [100] substrate with the excellent coverage.

The samples for TEM measurements were prepared by suspending the nanobelts (those are deposited at 500 °C) in ethanol (CH_3OH). After prolonged ultra-sonication few droplets of well dispersed solution were placed onto the standard carbon supported 600 mesh copper grid and drying slowly at room temperature. The typical bright field TEM micrograph at low magnification of

synthesized V_2O_5 NBs is shown in Fig. 4a. The low magnified bright field TEM micrographs of NBs confirming that nanobelts have well defined dimensions and possessing extremely large surface area because of their relatively larger open faces, can be seen in Fig. 4b. This makes V_2O_5 NBs specific for various technological applications such as storage device applications, display devices, and gas sensor devices with better efficiency. The dimensional analysis obtained by TEM observation is quite consistent with SEM results. Further the close examination of V_2O_5 nanobelts performed by HRTEM with selected area electron diffraction pattern divulges that every V_2O_5 nanobelts are composed of a single crystalline orthorhombic phase and the growth is oriented preferentially along [0 1 0] direction. In addition, the SAED pattern is recorded by focusing the electron beam perpendicular to the anisotropic growth axis of nanobelts, ascribed to [0 1 0] major zone axis diffraction as depicted in Fig. 4c, This exhibits diffraction spots with the d-spacing, which could be identified according to the orthorhombic crystal structure of V_2O_5 and also confirmed the single crystalline nature of V_2O_5 NBs with specific preferential orientation. This pattern does not alter as the electron beam moves along the nanobelts, suggesting the consistency of single crystalline nature of NBs along any directions. Fig. 4d displays a representative high resolution fringe pattern recorded from the highlighted region on arbitrarily chosen nanobelt. Parallel fringes with a spacing of 0.33 nm corresponding to [0 1 0] crystal planes can be easily detected, which is quite in agreement with the estimated spacing from XRD patterns. Several V_2O_5 NBs are investigated but they endorse approximately same results.

3.3. Compositional analysis using XPS

In order to investigate the material quality and relative composition, XPS analysis of V_2O_5 nanobelts grown at 500 °C in O_2-plasma is carried out. The survey scan plot of NBs obtained from this spectroscopic analysis is practicable to identify the elements exist on the film surface. Fig. 5a shows general XPS survey spectrum acquired from surface of V_2O_5 NBs, displaying only three intense bands of V (2p), O (1s), and C (1s) almost corresponding to the core level binding energies ($B.E_s$). The absence of other elements in the qualitative survey scan infers the compositional pureness of V_2O_5 NBs. In order to make our analysis more clear, the high resolution XPS spectrum of this sample is recorded, and de-convoluted with the best fitted six Gaussian peaks (P_1–P_6) corresponding to their $B.E_s$ 514.8 eV (P_1), 516.8 eV (P_2), 520.5 eV (P_3), 524.2 eV (P_4), 529.5 eV (P_5), and 531.5 eV (P_6), respectively as can be seen in Fig. 5b. In general, binding energies, chemical shifts, and FWHM associated with a particular peaks are primarily exploited for the samples analysis. There is a close relationship between

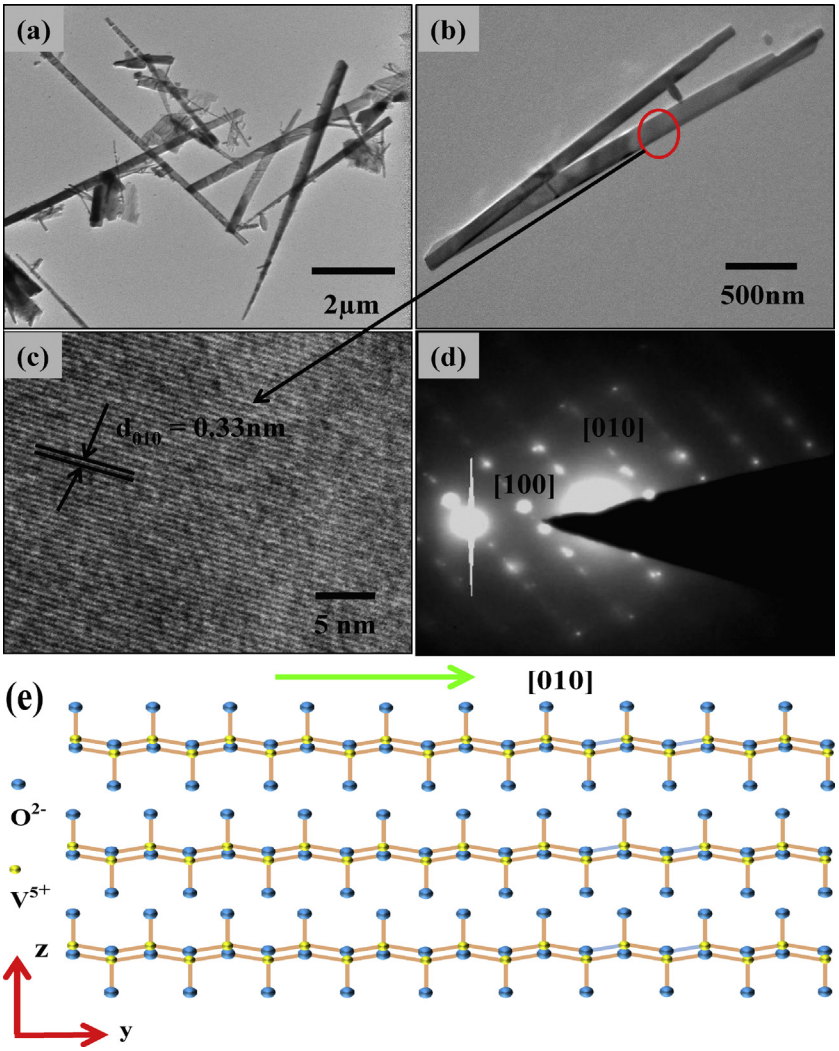

Fig. 4. Bright field TEM micrographs of V_2O_5 NBs particularly grown at 500 °C (a) at low magnification, (b) at higher magnification with the encircled region for HRTEM analysis, (c) typical HRTEM image of individual NBs with a fringe pattern, (d) SAED pattern recorded for a single belt and (e) atomic model of an orthorhombic phase of V_2O_5 with [0 1 0] growth direction.

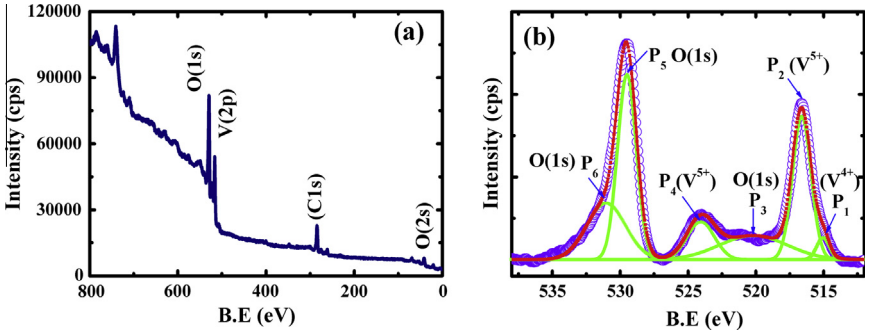

Fig. 5. XPS of the V_2O_5 nanobelts deposited at growth temperature 500 °C (a) survey spectrum and (b) Gaussian de-convoluted version of highly resolved spectrum of V (2p) and O (1s) bands ranging from 512 to 538 eV.

the core levels B.E and state of charge associated with the individual atom. It has been already established that increase in B.E of core levels result in an increase of positive charge on atom [17]. The recorded peaks P_2 and P_4 of V (2p) band positioned at 516.8 eV and 524.4 eV are corresponding to $V^{5+}(2p_{3/2})$ and $V^{5+}(2p_{1/2})$ doublet states respectively, with the typical spin orbit splitting of 7.4 eV, which matches with the reported value (see in Fig. 5b) [17]. It can be seen that FWHM of peak P_2 is relatively broader than P_4 due to the Coster-Kronig Auger transitions and well in consonance with the reported values [18]. The obtained results reveal that peak P_2 has a remarkable chemical shift of 4.8 eV to that of $V^{5+}(2p_{3/2})$ level of pure V-metal, located at about 511.95 eV corresponding to the highest oxidation state of vanadium. This observed shift is almost equal to the value as reported in literature [19]. Furthermore, both the resolved peaks P_2 and P_4 corresponding to V (2p) level have a small chemical shift of 0.5 eV compare to the value for pressed V_2O_5 powder [17]. This small shift as well as the appearance of a weak Gaussian peak P_1 at 514.8 eV corresponding to reduced oxidation state $V^{4+}(2p_{3/2})$ promising a slightly sub-stoichiometric nature of V_2O_5 NBs. The Gaussian peaks labeled as P_3 and P_5 are corresponding to O (1s) satellite peak of O^{2-} and O^- species respectively. The asymmetric nature of O (1s) band because of small shifting towards higher binding energy depicts the presence of chemisorbed hydroxyl –OH group (assigned by peak P_6) on surface of V_2O_5 film after deposition (see in Fig. 5b) [20].

3.4. Vibrational analysis

The vibrational properties of V_2O_5 NBs deposited on Si [100] substrate are systematically studied using IR and Raman spectroscopies in the spectral range of 400–2000 cm^{-1} and 100–1100 cm^{-1} respectively. The recorded IR reflectance spectrum of NBs shows several prominent absorption peaks positioned at 1605, 1450, 1008, 728, 572, and 470 cm^{-1} can be seen in Fig. 6. The absorption peaks lies between 400 and 1050 cm^{-1} as can be indexed according to distinct vibrational groups of V and O atoms coordinated in different ways. The analysis is based on the fact that V_2O_5 is formed by the distorted trigonal bi-pyramidal coordination polyhedra of O around V atoms for this coordination, stretching and bending vibrational IR active modes are invariably found in the range of 500–1200 cm^{-1}. The intense absorption peak situated at 1008 cm^{-1} is assigned to the stretching vibration of unshared V=O bond, which confirmed the presence of highest oxidation state V^{5+} in majority, whereas the relatively weak absorption peak located at 965 cm^{-1} shows the presence of V^{4+} oxidation state [21]. It is worth noting that the V=O stretching vibrational mode has a significant shift of ~15 cm^{-1} toward lower wavenumber from

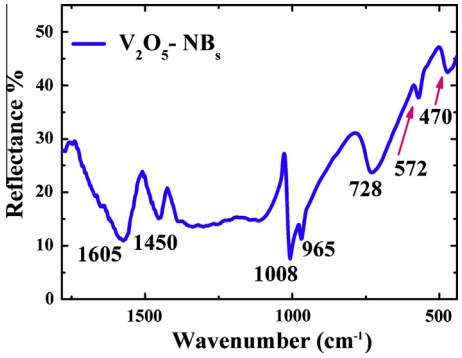

Fig. 6. FTIR spectra of finally grown V_2O_5 NBs.

the reported values, which suggests that V^{5+} is reduced into V^{4+} partially. The parallel attachment of the NBs (see in Fig. 3d) might be responsible significantly for this shift towards higher energy (see in Fig. 3d). The IR bands occupied in the range of 700–900 cm^{-1} is attributed to the anti-symmetric stretching vibration of the V—O_b—V group (O_b: bridge oxygen), in our case the peak for this vibrational mode is found at 728 cm^{-1} [22]. It is reported earlier that the group of bands presented at wavenumber < 600 cm^{-1} corresponding to the edge shearing 3V—O_c (O_c: threefold coordinated oxygen atom) bridge oxygen stretching and the bridging V—O_b—V deformations [23]. In the observed IR spectrum, the peaks located at 572 and 470 cm^{-1} are corresponding to these vibrational modes and in accordance with the reported values. In addition, two additional less intense peaks positioned at 1605 and 1450 cm^{-1} corresponding to -OH bond are due to the hydroxylation of film surfaces [21] while taking it out of vacuum chamber, which reveal the presence of adsorbed free water molecules on film.

Fig. 7 shows the details of Raman bands of V_2O_5 NBs with the vibrational bands located at 147, 194, 280, 405, 478, 525, 695,

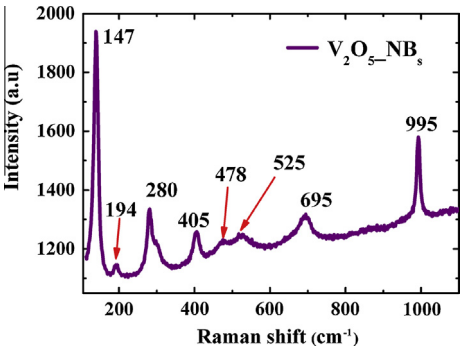

Fig. 7. Micro-Raman spectrum of V_2O_5 NBs deposited at 500 °C in O_2-plasma.

and 995 cm^{-1}, which is assigned the characteristic vibrational modes of polycrystalline orthorhombic phase of V_2O_5. The obtained Raman bands are shifted slightly towards lower wave number than reported values, which manifests that V_2O_5 NBs deviates from its perfect stoichiometry ratio. Among all the peaks, the most intense peak obtained at 147 cm^{-1} is attributed to the skeleton bent vibration (B_{3g}), while relatively less intense peaks located at 194 and 280 cm^{-1} are corresponding to the bending vibrations of O_c—V—O_b bonds (A_g and B_{2g} modes) [24]. The bending vibrational mode in V—O_b—V (A_g) entity and the stretching vibration of V—O_c (B_{2g} mode) bond are predominantly observed at 405 and 695 cm^{-1} [24,25]. It is reported earlier [24] that the layered structure found in V_2O_5 is stacked up from the distorted trigonal bi-pyramidal coordination polyhedra of oxygen atoms around vanadium atoms. The edge sharing of distorted trigonal bi-pyramidal atoms form $(V_2O_4)_n$ zigzag double chains along the (001) direction and cross-linked along (100) direction through the corner sharing. It is observed that vanadyl oxygen is easily removed from the surface result in the cleavage of [001] planes and vacancies are left behind in ordered distribution. The skeleton bent mode centered at 147 cm^{-1} is evidenced the layer-like structure of V_2O_5 films. Moreover, the peak located at 995 cm^{-1} is associated with the vanadyl mode corresponding to the stretching of vanadium atoms connected to oxygen atoms by double bonds, and also signify the layered structure of V_2O_5 film [13]. The less prominent peak located at 525 cm^{-1} is assigned to the triply coordinated oxygen atom V_3—O, which is formed by the edge-shared oxygen atoms in three pyramids [22].

3.5. Photoluminescence studies

Room temperature PL emission of V_2O_5 NBs is recorded in the wavelength range from 450 to 725 nm having the excitation wavelength of 325 nm (3.81 eV) more than the band gap of V_2O_5. The de-convoluted version with the best Gaussian fit is shown in Fig. 8. The main peak is focused at 565 nm (2.19 eV), which is quite consistent with the reported band gap of polycrystalline V_2O_5 film (~2.3 eV), which affirming the enhanced emission would mainly owing to the near band edge emission in V_2O_5 NBs. The PL emission peak positioned at 650 nm (1.94 eV) is assigned the presence of oxygen defects in V_2O_5 NBs grown at 500 °C [17,26]. The occurrence of intense PL emission mainly in visible regime assured better degree of crystallinity as have been shown by SEM and XRD outcomes as well. In our observation the band gap is slightly shifted toward lesser energy value than the reported value, which is principally due to the appearance of oxygen defect levels in band gap. It is reported that the Fermi level in V_2O_5 is positioned between the gap of V (3d) and O (2p) bands [27]. The existence of layered structure in α-V_2O_5 is being the cause of splitting of V(3d) conduction band, this splitting in V (3d) level will localize a band shift ~0.6 eV below than its original value [28]. This might

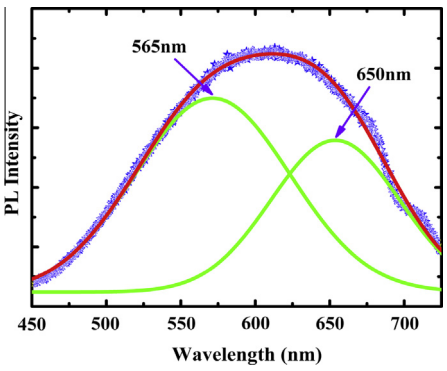

Fig. 8. Gaussian de-convoluted form of PL spectra of V_2O_5 NBs with two peaks.

be assigned to a different electronic structure and conducting to the complete transitions between V (3d) split-off bands. These transitions actually favor the radiative transitions between the split-off band and O (2p) band. Thus the emission corresponding to the band of energy 2.19 eV could be explained by the radiative transitions between the V (3d) and O (2p) bands [28].

3.6. Growth mechanism

In order to understand the complete growth of V_2O_5 NBs deposited on Si wafer in oxygen plasma without any catalytic layer, the surface morphologies of films deposited at distinct growth temperatures with and without oxygen plasma are recorded using SEM as shown above. In general, vapor–solid (VS) and vapor–liquid–solid (VLS) approaches are well known, to explicate the growth of nanostructures using several physical vapor deposition (PVD) routes [29,30]. Moreover, the reaction kinetics of oxygen plasma is also well known. In present work, the growth of α-V_2O_5 NBs likely adopts the solidification through vapor–solid approach because no catalyst is required for this growth. This catalyst free growth scheme may be provided for one dimensional nanostructured growth of cubic crystal structure as well as anisotropic crystal structure materials. The primary advantage of catalysts free route is that, it completely omit the possibility to incorporate the catalytic impurities in sample [31], which might be take place during condensation–precipitation process in metal catalysts-assisted VLS growth mechanisms, result in the formation of high purity of V_2O_5 nanobelts as investigated by structural and compositional analysis. In this study the main source of material is the vaporized V_2O_5 molecular species prepared during the thermal oxidation of vanadium metallic strip in O_2 -plasma at growth temperature of 500 °C. The entire growth process is supposed to be modeled in three successive steps and the schematic representation is shown in Fig. 9. The first (i) growth step executes the formation of V_2O_5 molecules (which may not be in perfect stoichiometry) on vanadium metal during oxidation and their arrival on Si substrates after detaching from V-strip. Second step (ii) initiates with the formation of nuclei with the coordination of sub-stoichiometric oxides, finally (iii) the last step includes the formation of V_2O_5 nanobelts on these nuclei over entire substrate in uniform fashion. It has reported earlier [32] that O_2-plasma is mainly composed of electron (e^-), positive and negative oxygen ions, neutrals, and many other excited metastable states of oxygen molecules. These energetic ionic species of oxygen in plasma behaves as the strong oxidizing regent during oxidation of V-metal into V_2O_5. Many techniques and models such as Langmuir probe technique, fluid model, and tandem mass spectrometer are employed to identify the variety of oxygen ionic species in O_2-plasma with the interpretation of reaction kinetics [32,33]. According to these models, O_2^+ is most prevalent positive ion compare to the other species at low pressure because it is relatively easy to remove electrons from an oxygen molecule [15,34]. The major negative ions in oxygen plasma are O^-, O_3^- and electrons, whereas pre-dominant neutral is O_2 [32,33]. Among these species electrons and O^- ions in oxygen plasma are most crucial species to stimulate the growth of V_2O_5 on V-surface [15]. The expected growth of V_2O_5 film on V-metal during thermal oxidation is given in terms of following equations:

$$2V + 5O^- \rightarrow V_2O_5 + 5e \quad (1)$$

$$2V + 5/2O_2^+ + 5e \rightarrow V_2O_5 \quad (2)$$

$$2V + 2O_3^- \rightarrow V_2O_5 + O^- + 5e \quad (3)$$

Equations (1) and (2) are supposed to be most probable oxidation reaction to obtain V_2O_5 on the surface of vanadium during the

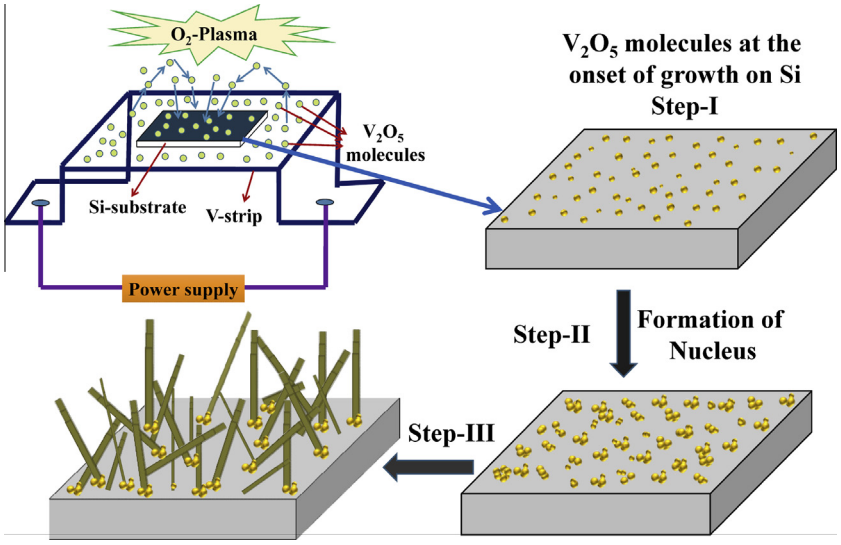

Fig. 9. Schematic representation of proposed growth model to grow V_2O_5 NBs in three consecutive steps.

thermal oxidation, owing to the prominent number density of O^- and O_2^+ ions in oxygen plasma [33]. Third reaction has relatively less contribution in oxidation process due to the low concentration of O_3^- ions in plasma. Other oxygen species (ionic as well as neutral) have comparatively lesser concentrations in plasma. Still these species facilitate in the conversion of V into V_2O_5 but their contributions are not significant. Besides that, the deposition at relatively low temperature in O_2-plasma is not relevant for the growth of NBs on Si substrate, as can be seen in Fig. 2a and b. Low growth temperature leads to less molecular mobility on substrates, because of this V_2O_5 molecules could not properly migrate on substrate to attain minimum energy nucleation sites consequently, no structure with well-defined features would develop on Si wafer. Therefore, the proper combination of growth temperature with O_2-plasma (such as 500 °C in our case) is most required to deposit V_2O_5 NBs with the large scale of coverage. Furthermore, it is assumed that vanadium oxide molecules arriving on substrate surface at very initial stage are composed of sub-stoichiometric cation–anion molecules as observed through experimental results as well [35]. When the condensation is carried out on substrate at 500 °C during onset of growth, these anion and cation coordination is upheld to balance the local charge as well as structural symmetry, consequently small number of nuclei are commence to formed (Fig. 9). The freshly arriving V_2O_5 molecules will continue sitting on these nuclei, while the surfaces that have lower surface energy start to form such as some side surfaces [35]. The low melting point of V_2O_5 (~700 °C) furnishes uninterrupted supply of V_2O_5 molecular flux after oxidation, result in a continuous volatilization of V_2O_5 molecules are carried out from V-metal surface to substrate. Since, during the growth substrate is kept at 500 °C, which will provide sufficient thermal energy to the impinging V_2O_5 molecules when reaching on to substrate. This additional energy is sufficient to move on Si substrate to attain lower surface energy sites. This would help the low energy surfaces tending to be flat with their expansion in surface area as more and more molecules affix on rough surface fronts. As the time passes, large number of V_2O_5 molecules would affix on growth fronts as well as on the side edges, but the smoothness of side surfaces and relatively high molecular mobility precluded them to remaining on the surfaces of NBs. Consequently, these molecules diffuse randomly on substrate and finely obtained the lower energy sites on growth fronts and favored the growth of NBs of very high aspect ratio (see in step III). In addition, the oxygen vacancies particularly on the top edges of belts render the nucleation sites for further growth and strongly reduce the barrier for incorporation of incoming V_2O_5 vapor flux on top of NBs. The obtained results endorse that rough structure of nanobelts tip is the signature of fast accumulation of V_2O_5 molecules, which is also a signature of the rapid growth of NBs along the direction of their tips, as can be seen in Fig. 3d. It is worth noting that the existence of intense field because of high potential difference across electrodes during growth is effectively guiding the in coming V_2O_5 molecules on entire substrate to enhance the coverage density and facilitates them to grow preferentially along [010] direction as well. As for as the alignment of NBs is concerned, significant difference in close packing along [010] and [100] crystal plane in α-V_2O_5 led to the remarkable difference in growth rates in these crystal directions. From the energy point of view *b*-axes is most preferred direction for the growth of one dimensional nanostructure. Hence, the NBs aligned preferentially along (010) direction is formed with very large aspect ratio (see in step III). As reported earlier [2] that temperature gradient between the source (V-metal strip) and surface of substrate also helps the growth of one dimensional nanostructure. In this case, the temperature gradient after 30 min is found to be ~50 °C because of increase in film thickness and is favorable for the growth of V_2O_5 NBs. More interestingly, the close examination of film endorse that NBs are not individual but in the form of parallelly aligned bunches of NBs through the oriented attachment of adjacent nanobelts. It is conceived that the NBs are formed bunched may be due to strong surface interactions, when more than one parallel nanobelts come in close proximity, as can be seen in inset of Fig. 3d. These surface interactions mainly exist owing to the presence of unsaturated bonding on the open faces of NBs [36]. In principle, there is no restriction either on the number of NBs or on their directions of alignment during bunch formation. All studies confirmed the fabrication of α-V_2O_5 NBs on the Si [100] substrate with enhanced coverage density, effectively offers very large reactive surface area, this distinctly categorized as a fascinating candidate from the device applications point of view such as in secondary lithium ion batteries, gas sensor, and electrochromic devices.

4. Conclusions

In summary, we have demonstrated the growth of V_2O_5 nanobelts on Si substrate employing an effective and simple PVD route namely plasma assisted sublimation process (PASP) without any templates and catalysts for the first time to the best of our knowledge. Oxygen

plasma is used as an active medium during deposition and must be needed to grow NBs particularly when growth temperature is maintained 500 °C. The observed results endorsed that low temperature during growth even in presence of O_2-plasma is not appropriate for the formation of NBs. While in a simple oxygen gas without exciting plasma, no film is deposited on substrate. The morphological and structural studies of film prepared at 500 °C in O_2-plasma confirmed the growth of NBs with high coverage density with single orthorhombic phase. The magnified view depicts that nanobelts are not individual but in the form of bunches, which is because of some surface interactions. Further investigations of NBs are carried out by HRTEM with SAED revealing the single crystalline nature of V_2O_5 NBs with the fringe width of ~0.33 nm measured along (0 1 0) direction. The sharp and considerably intense Raman as well as IR bands are assigned different vibrational modes of V—O binding system. The XPS results of NBs ensuring the purity of NBs with their sub stoichiometric nature. Vanadium pentoxide NBs are exhibit intense photoluminescence emission at room temperature with two prominent peaks located at 565 and 650 nm, further assuring the sub-stoichiometric nature of NBs. In this paper, a vapor solid (VS) strategy to the growth of α-V_2O_5 NBs has been proposed in detail. All the observed results are well in consonance with each other.

Acknowledgement

One of the authors Rabindar K. Sharma gratefully acknowledges the financial assistance from Council of Scientific and Industrial Research (CSIR)-India.

References

[1] Zu Rong Dai, Zheng Wei, Zhong L. Wang, Adv. Funct. Mater. 13 (2003) 9.
[2] K. Rabindar, G. Sharma, B. Reddy, J. Phys. D: Appl. Phys. 47 (2014) 065305.
[3] A. Dhayal Raj, T. Pazhanivel, P. Suresh Kumar, D. Mangalaraj, D. Nataraj, N. Ponpandiana, Curr. Appl. Phys. 10 (2010) 531.
[4] Tianyou Zhai, Haimai Liu, Huiqiao Li, Xiaosheng Fang, Meiyong Liao, Lang Li, Haoshen Zhou, Yasuo Koide, Yoshio Bando, Dmitri Golberg, Adv. Mater. 22 (2010) 2547.
[5] Olga B. Lapina, Alexander A. Shubin, Andrei V. Nosov, J. Phys. Chem. B 103 (1999) 7599.
[6] Xiao-Fei Zhang, Kai-Xue Wang, Xiao Wei, Jie-Sheng, Chem. Mater. 23 (2011) 5290.
[7] Keng-Che Cheng, Fu-Rong Chen, Ji-Jung Kai, Sol. Energy Mater. Sol. Cells 90 (2006) 1156.
[8] Yuqan Wang, Zhengjun Zhang, Physica E 41 (2009) 548.
[9] S. Beke, S. Giorgio, L. Korosi, L. Nanai, W. Marine, Thin Solid Films 516 (2008) 4659.
[10] C. Julien, E. Haro-Poniatowski, M.A. Camacho-López, L. Escobar-Alarcon, J. Jımenez-Jarquın, Mater. Sci. Eng. B65 (1999) 170.
[11] C. Diaz-Guerra, J. Piqueras, J. Appl. Phys. 102 (2007) 084307.
[12] Xianhong Rui, Ziyang Lu, Zongyou Yin, Dao Hao Sim, Tuti Mariana Lim, Huey Hoon Hng, Hua Zhang, Qingyu Yan, Small 9 (2013) 716.
[13] Tianyou Zhai, Haimei Liu, Huiqiao Li, Xiaosheng Fang, Meiyong Liao, Liang Li, Haoshen Zhou, Yasuo Koide, Yoshio Bando, Dmitri Golberg, Adv. Mater. 22 (2010) 2547.
[14] P. Lim, J.D. Long, S. Xu, K. Ostrikov, J. Phys. D: Appl. Phys. 40 (2007) 1085.
[15] Rabindar K. Sharma, G.B. Reddy, J. Appl. Phys. 114 (2013).
[16] Rabindar K. Sharma, G.B. Reddy, AIP Adv. 3 (2013) 092112.
[17] A.Z. Moshfegh, A. Ignatiev, Thin Solid Films 198 (1991) 251.
[18] E. Antonides, E.C. Janse, G.A. Sawatzky, Phys. Rev. B 15 (1977) 4596.
[19] J. Kasperkiewicz, J.A. Kovacich, D. Lichtman, J. Electron. Spectrosc. Relat. Phenom. 32 (1983) 123.
[20] A.Z. Moshfegh, A. Ignatiev, Surf. Sci. Lett. 275 (1992) L650.
[21] Yupin Chen, Gang Yang, Zihui Zhang, Xioaoyan Yang, Wenhua Hou, Jun-Jia Zhu, Nanoscale 2 (2010) 2131.
[22] C. Julien, G.A. Nazri, O. Bergstrom, Phys. Status Solidi B 201 (1997) 319.
[23] Angela SĬurca, Boris Orel, Electrochim. Acta 44 (1999) 3051.
[24] Q. Su, C.K. Huang, Y. Wang, Y.C. Fan, B.A. Lu, W. Lan, Y.Y. Wang, X.Q. Liu, J. Alloys Comp. 475 (2009) 518.
[25] Se-Hee Lee, Hyeonsik M. Cheong, Maeng Je Seong, Ping Liu, C. Edwin Tracy, Angelo Mascarenhas, J. Roland Pitts, Satyen K. Deb, Solid State Ionics 165 (2003) 111.
[26] Bin yan, Lei Liao, Yumeng You, Xiaojing Xu, Zhe Zheng, Zhe Zheng, Zexiang Shen, Jan Ma, Limin Tong, Ting Yu, Adv. Mater. 21 (2009) 2436.
[27] Ming Li, Fengyu Kong, Hongqiang Wang, Guanghai Li, Cryst. Eng. Commun. 13 (2011) 5317.
[28] Walter Lambrechttt, Bahram Djafari-Rouhani, Joost Vennik, J. Phys. C: Solid State Phys. 19 (1986) 369.
[29] J.W. Dailey, J. Taraci, T. Clement, D.J. Smith, J. Drucker, S.T. Picraux, J. Appl. Phys. 96 (2004) 7556.
[30] D. Yuvaraj, K. Narasimha Rao, K. Barai, Solid State Commun. 149 (2009) 349.
[31] R.S. Wagner, W.C. Ellis, Appl. Phys. Lett. 4 (1964) 89.
[32] X.D. Liu, J.A. Yang, H.X. Wang, Z.M. Rong, F. Iza, G.M. Kong, J. Phys. D: Phys. 45 (2012) 305205.
[33] Y. Ichicawa, C.R.L. Wu, T. Kaneda, J. Appl. Phys. 67 (1990) 108.
[34] Y. Itikawa, Phys. Fluids 16 (1973) 831.
[35] Zu Rong Dai, Zheng Wei Pan, Zhong L. Wang, Adv. Funct. Mater. 13 (2003) 9.
[36] Y. Li, J. Liu, H. Xintang, G. Li, Cryst. Growth Des. 77 (2007).